Observation of a Continuous Spectral Shift in the Solvation Kinetics of Electrons in Neat Liquid Deuterated Water

C. Pépin, T. Goulet, D. Houde,* and J.-P. Jay-Gerin

Département de médecine nucléaire et de radiobiologie, Faculté de médecine, Université de Sherbrooke, Sherbrooke, Québec, Canada J1H 5N4

Received: January 29, 1997; In Final Form: April 2, 1997[⊗]

Multiphoton ionization of neat liquid D_2O at room temperature (295 K) with 2-eV subpicosecond laser pulses is used to study the solvation of electrons in this medium. The set of 20 measured kinetic traces covers a wide range of probing wavelengths (450−1450 nm), which allows us to obtain a global picture of the spectral changes that accompany electron hydration. The construction of transient absorption spectra from a proper normalization of the kinetic traces confirms the well-known existence of two absorbing species, one weakly bound absorbing chiefly in the infrared and a strongly bound one whose spectrum at long times is that of the well-characterized hydrated electron. The transient spectra also reveal the occurrence of a stepwise transition between these two species as well as a concomitant continuous blue shift of the strongly bound electron−solvent configuration. A nonlinear fit performed simultaneously on all the data allows the estimation of the characteristic kinetic and spectral parameters of our previously proposed hybrid model of electron solvation when it is applied to D_2O. The global fit closely matches the data for the 20 different probing wavelengths investigated. The electrons are found to get trapped in 0.16 ± 0.02 ps, whereas the stepwise transition and the continuous blue shift characteristic times are 0.41 ± 0.02 and 0.51 ± 0.03 ps, respectively. The extent in energy of the monoexponential blue shift of the strongly bound electron spectrum is 0.34 ± 0.02 eV, a value which is very similar to the one that was found for electron solvation in methanol. Finally, it is estimated that about 34% of the electrons get directly trapped into the strongly bound state.

1. Introduction

Over the last decades, many experimental[1−39] and theoretical[40−61] studies have been devoted to elucidate the physical mechanisms underlying the solvation of electrons in polar liquids. In the case of electron solvation in water (hydration), the molecular relaxation time is so fast (less than 1 ps) that its direct observation only became feasible with the advent of femtosecond pulsed laser photolysis.[14−17,19−28,30−38]

In spite of these numerous studies on electron hydration, this process still remains incompletely explained owing mainly to the fact that it can only be unveiled through a temporal deconvolution of the observed transient absorption signals. Its various modelings, which have largely been inspired by the (slower) solvation of electrons in alcohols,[2−10,12,13,18,26,29,31,35,36,39] all agree on the involvement of a stepwise transition between two species, one absorbing chiefly in the infrared that we may generally describe—from an energetic standpoint—as being "weakly bound" (e^-_{wb}) and a "strongly bound" one (e^-_{sb}) that absorbs in the visible and whose spectrum at long times is that of the well-characterized fully hydrated electron (e^-_{aq}). It is also widely admitted that the electrons do not have to create their trap sites since a large number of those fluctuating states are readily available to them in polar media.[12,43,45,62−64] Nevertheless, major controversies are still present in this field. They concern mainly (i) the observation of an isosbestic point in the transient spectra,[14,19,24,37,48,50] (ii) the existence of a direct solvation channel that would allow the electron to avoid transiting through the e^-_{wb} state,[12,13,26,31,37,48,50,53,54,56] (iii) the existence of a supplementary absorbing species in the near infrared associated with transient encounter pairs,[20,24,27,38] (iv) the role played by a continuous relaxation of the solvent in the spectral evolution of the absorbing species,[14,18,28−31,36,40−42,44,46−48,50,51,53,55,57] and (v) the absorption of visible or near infrared light by quasi-free electrons prior to their trapping.[53,54,56]

In previous studies,[31,36] we found that the solvation of electrons in liquid methanol involves more than a strictly stepwise transition between e^-_{wb} and e^-_{sb}. We showed that the collection of kinetics reveals a continuous blue shift of the absorbing species taking place concurrently (though at a slower rate) to the stepwise transition between them. Our set of kinetic traces were successfully fitted[36] with a model that we called "hybrid" owing to the fact that it involves those two types of relaxation of the electron−solvent configurations. In the course of these studies, we found that a clear understanding of the electron solvation in methanol could only be achieved by the measurement of transient absorption kinetic traces over a wide range of probing wavelengths and by the confrontation of the models to the entire collection of these data.

In this paper, we present a new set of 20 individual kinetic traces that we measured at 50-nm intervals between 450 and 1450 nm (except at 600 nm) in liquid D_2O and examine them to see whether or not the mechanism of electron hydration differs qualitatively from that of solvation in alcohols. The choice of deuterated water was dictated by our attempt to detect the e^-_{wb} as far as possible beyond 1000 nm, a spectral region where D_2O absorbs much less than H_2O. Using the kinetic traces, we reconstruct a series of transient spectra that directly illustrate the existence of the two absorbing species mentioned above. These transient spectra also reveal the occurrence of a stepwise transition between the two species and a continuous shift of the e^-_{sb} spectrum. In an effort to quantify the various aspects of

* To whom correspondence should be addressed. E-mail: dhoude@courrier.usherb.ca.

⊗ Abstract published in *Advance ACS Abstracts,* May 15, 1997.

S1089-5639(97)00354-X CCC: $14.00

the observed spectral changes, we perform a simultaneous fit on all these data using our hybrid solvation model.

2. Experiment

Electrons are directly ejected from the solvent molecules with 2-eV laser pulses by a multiphoton ionization process which was shown to provide a high yield of solvated electrons.[25,30] The powerful (∼0.5 mJ) and short (∼300 fs) pump pulses are produced with a colliding pulse mode-locked (CPM) dye laser followed by four stages of amplification in kiton red and rhodamine filled cells pumped by a 10 Hz Nd:YAG laser operated at 532 nm. The probe, originating from the same pulse as the pump, covers a wide range of wavelengths after the passage of the pulse through a continuum-generating D_2O cell. At wavelengths greater than 1300 nm, the (101) absorption band of H_2O is sufficiently intense to impair the detection of generated photons whereas the corresponding combination band of heavy water lies close to 2000 nm. Unfortunately, sufficient signal amplitudes could not be attained beyond 1500 nm. Narrow band-pass and neutral density filters were used to reduce to a minimum the amount of probe light striking the cell. In order to counter systematic amplitude drifts, a shot selection scheme was implemented. For a particular shot to be accepted it must lie within a specified intensity window which is set before the recording of a kinetic trace and which remains constant thereafter. A chopper intercepts the pump beam so that light absorption with and without exposure to the exciting pulse is alternately monitored to ensure that a change in their ratio is solely attributable to events induced by the 2-eV photons.

Focusing optics allowed an irradiance of $\sim 10^{17}$ W/m^2 inside a 5-mm Suprasil quartz cell filled with D_2O at 295 K. An upper limit for the duration of the pulses inside the sample was found to be 420 fs (full width at half-maximum) from the observation of transient Raman signals.[30] The certified minimum isotopic purity of the deuterium oxide provided by MSD Isotopes was 99.9 atom % D. Single-channel traces were collected with silicon photovoltaic diodes below 800 nm, whereas germanium photodiodes were used for detection in the infrared. A small amount of light arising from the continuum generated inside the sample cell by the pump pulse could be observed. Since the consequence of this effect is to create a constant negative absorbance base line, it could easily be discriminated from the transient signal.

The presence of the high electric field (a few gigavolts/meter) may raise the question of a possible dielectric breakdown in the sample. This phenomenon was ruled out after conducting a test with gradually decreasing pump powers (down to a factor of 10). The slope of the resulting absorbance curve remained constant throughout, without showing any sign of the sudden deviation that would result at the onset of dielectric breakdown. Moreover, its characteristic light flashes were not observed in the cell.

It has been argued that long sample cells (5 mm) would make the system response significantly slower and distort the system response function from the original shape of the laser pulse.[35] In another paper on electron hydration, McGowen *et al.*[32] have focused their 3.2-eV pump beam on a 100-μm flow jet. Beforehand they had performed experiments in a 10-mm path length cuvette and found the results identical except for a "slightly poorer" resolution but a larger signal size. When changing from a 2-mm to a 5-mm cuvette, we also observed superimposable kinetic traces and consequently opted for the latter cell because higher electron yields could be generated and the signal could be observed farther in the infrared than ever before in spite of a small degradation of the time resolution.

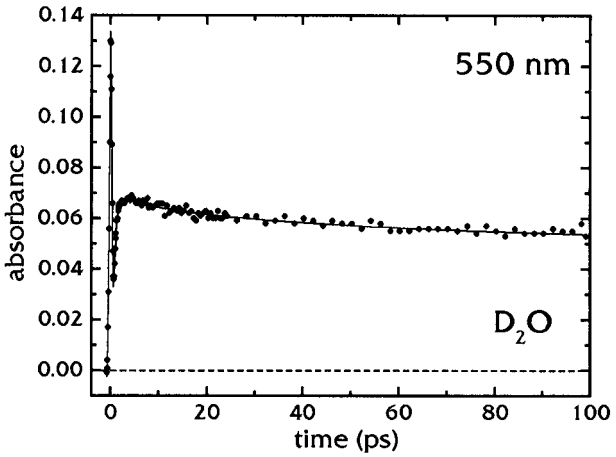

Figure 1. Variation over a large time range of the measured absorbance in liquid D_2O at 295 K for a probing wavelength of 550 nm. The monotonic decay is caused by the geminate recombination of the partially and fully hydrated electrons with the ions D_3O^+ and the radicals OD. The strong absorption at time zero is due to an inverse Raman effect. The solid line is the result of the overall fit which was performed simultaneously on the 20 experimental kinetic traces (see text).

3. Results

3.1. The Measured Kinetic Traces. Figure 1 illustrates the fact that, on a time scale of a few tens of picoseconds, the measured absorbance decreases monotonically owing to the geminate recombination of partially and fully hydrated electrons with OD and D_3O^+. This phenomenon, which is observed uniformly over the whole spectral range investigated, is well characterized by the Monte Carlo simulation of the diffusion and encounter kinetics of these species.[65] We used the distribution [$f(r) \propto r^2 \exp(-r/b)$] of initial separations r between the electrons and the pair OD−D_3O^+ which is the most appropriate for a few-step random walk.[65,66] In this case, the mean value of r was found to be 1.6 nm. To facilitate the inclusion of the recombination into the convolution of the pump and probe pulses, we describe the survival probability of an ejected electron with the following function: $\Omega(t) = 0.702 + 0.022 \exp(-t/1.48) + 0.073 \exp(-t/10.18) + 0.2 \exp(-t/76.4)$, which fits very well the numerical results (the times are given in picoseconds). It has been shown that the recombination kinetics depends on the energetics of the photoionization[32,67,68] and is thus specific for each experiment.[15−17,22,23,25,26,32,37,38,65,67−69] We should mention here that, contrary to what was found[22] in experiments where 4-eV photons are used to ionize water, the recombination kinetics that we observe is unaffected by a 10-fold attenuation of the pump pulse intensity.

Figure 2 displays 6 of the 20 measured kinetic traces in liquid D_2O between 450 and 1450 nm. In order to clearly identify the contribution of the hydration kinetics to the observed variations of absorbance, we display the slow decay that results from the recombination alone. Beyond 2.5 ps, the observed kinetic traces of most probing wavelengths merge into the recombination survival function, indicating that the hydration process is essentially completed by that time. An exception to that behavior is seen at 950 nm where an excess of absorption is observed to last significantly longer. Between 0.5 and 2.5 ps, there is a steady rise in absorbance for probe wavelengths equal to 550 and 650 nm, whereas for longer wavelengths, the rise is faster and followed by a decay. As for the structures observed around zero time delays, they are due to various nonlinear phenomena related to the interaction between the pump and the probe pulses. They will be further explained in section 4.1. For now, we can mention that they prove to be

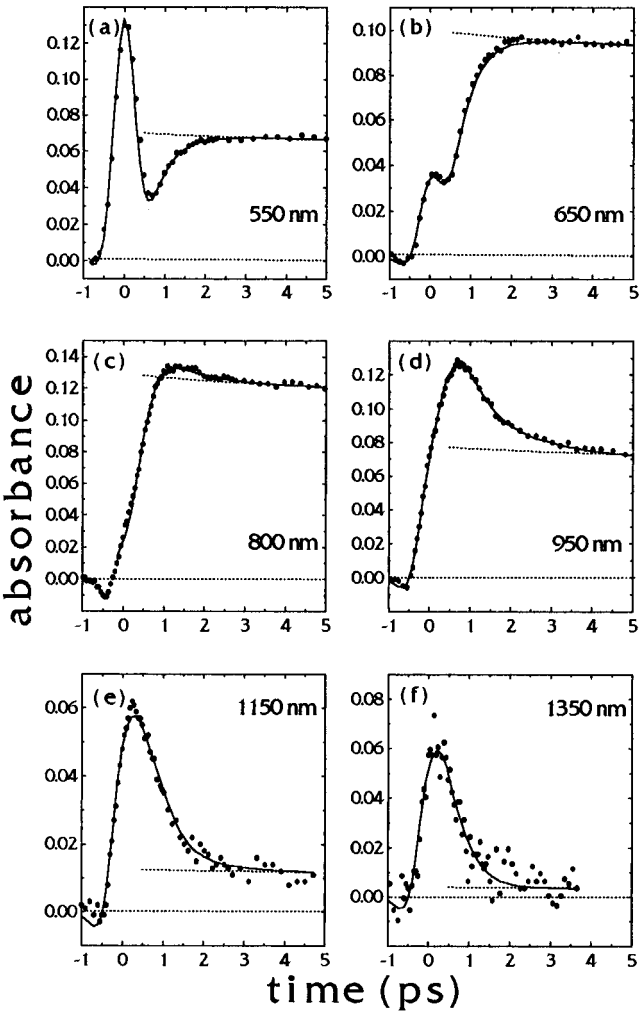

Figure 2. Variation with time of the observed (not normalized) absorbance in liquid D_2O at 295 K for 6 of the 20 probing wavelengths considered in this study. The solid lines are the result of the overall fit which was performed simultaneously on the 20 experimental kinetic traces (see text). The dashed lines represent the variation of absorbance that would result from the sole process of geminate recombination. These survival-probability curves are scaled to merge into the fitted kinetics at 5 ps for (a)−(d) and at the longest observed absorbances for (e) and (f).

useful for determining the position of delay zero (the coincidence of the pulses).

The experimental kinetic traces shown in Figures 1 and 2 are all accompanied by a solid line that results from a fit performed simultaneously for all the studied wavelengths. The details of the fitting procedure and of the underlying model will be given in section 4. One can note that the fits are all very good and that the signal-to-noise ratio of the data is quite large, especially in the case of wavelengths below 1150 nm for which the probe pulse is more intense. The kinetic traces shown here have not been normalized, and variations of intensity from one wavelength to another result from both the changes in the extinction coefficients of the absorbing species and in the experimental conditions (power of the pump pulse, overlap volume of the probe and the pump in the sample, etc.).

3.2. Construction and Analysis of the Transient Spectra. The scaling of the measured absorbances is necessary when we wish to construct the transient spectra. For the major part of the studied spectral region, this normalization can be done with the help of the known e^-_{aq} absorption spectrum[70] that we observe in the long-time limit of our experiment. For the longer

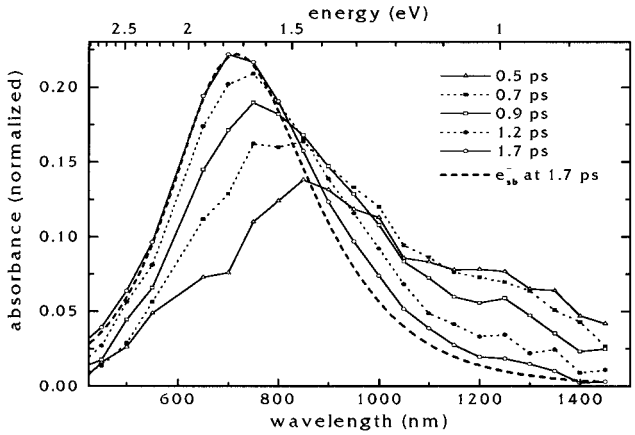

Figure 3. Transient absorption spectra of excess electrons in liquid D_2O at 295 K for five time delay values between the pump and the probe pulses. The absorbances have been normalized (see text) to account for differences in the experimental conditions from one probing wavelength to another. The slow decay due to the geminate recombination has not been removed from those spectra. The dashed curve is a Gaussian−Lorentzian function whose width is that of the fully hydrated electron and which has been scaled and displaced to the red (by 0.024 eV) to fit the visible part of the 1.7-ps transient e^-_{sb} spectrum. The error bars are not shown for the sake of clarity but are of the order of ±0.005 below 1100 nm and ±0.01 above this probing wavelength.

probing wavelengths, however, the extinction coefficient of e^-_{aq} is too small and this procedure becomes unreliable. The normalization above 1000 nm was achieved by a calibration of the evolution of the transient absorption peaks below this limit wavelength and a subsequent extrapolation of its behavior beyond 1000 nm.

Figure 3 displays the transient spectra that we constructed from the observed kinetics. For each wavelength, an average was calculated over the values of the optical densities measured at delays close to the selected one. Note that, here, the optical densities are normalized and the absorption or emission structures around delay zero have been subtracted. One readily sees that at least two species contribute to the absorption: one best seen at early times which seems to peak between 1200 and 1300 nm and the other—absorbing chiefly in the visible—that shifts gradually toward shorter wavelengths and whose amplitude increases with time. The fact that the buildup in the visible can be correlated to the decay in the infrared constitutes the basis on which it has been suggested that the process of hydration consists essentially of a stepwise transition between a weakly bound species (e^-_{wb}) and a strongly bound one (e^-_{sb}).[14,19] However, it also appears clearly here that this major feature of the spectral evolution associated with the hydration of electrons is accompanied by a continuous blue shift (of a few tenths of an electronvolt) of the e^-_{sb} spectrum. The dashed curve that we added to Figure 3 illustrates that, on one hand, the visible part of the transient spectrum at 1.7 ps essentially coincides with a fully hydrated electron spectrum which is displaced to the red by a mere 0.024 eV. It thus seems that the blue shift is almost completed by that time. Also completed is the decay of the e^-_{wb} species which can be monitored above 1100 nm. On the other hand, the 1.7-ps transient absorption spectrum exhibits a significant excess in the range 900−1100 nm. This excess, which is observable up to ∼4 ps, is the spectral manifestation of the longer relaxation that was noted in Figure 2d.

In order to characterize the blue shift and the buildup of the e^-_{sb} spectrum, we monitored at every 100 fs the evolution of the transient spectrum from the shortest probed wavelengths to those

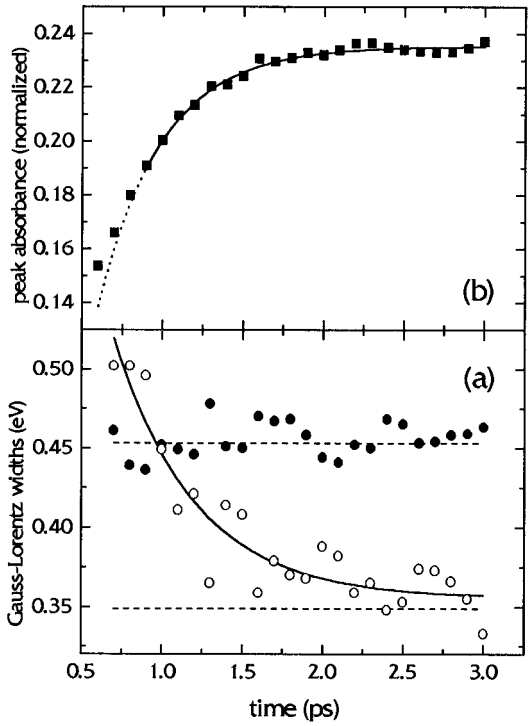

Figure 4. (a) Variation with time of the half-widths at half-maximum (hwhm) of the Gaussian−Lorentzian functions that have been used to fit the observed transient spectra. (○) hwhm on the Gaussian (red) side. (●) hwhm on the Lorentzian (blue) side. The dashed lines indicate the values of the hwhm for the fully hydrated electron in D_2O (ref 70). (b) Variation with time of the height of the Gaussian−Lorentzian functions that have been used to fit the observed transient spectra. Note here that the effect of the geminate recombination on the height has been taken into account. The solid line represents an exponential function, with characteristic rise time equal to 0.39 ps, which was fitted through the data points from 0.9 to 3.0 ps. The dotted curve is the extrapolation of this function to shorter time delays.

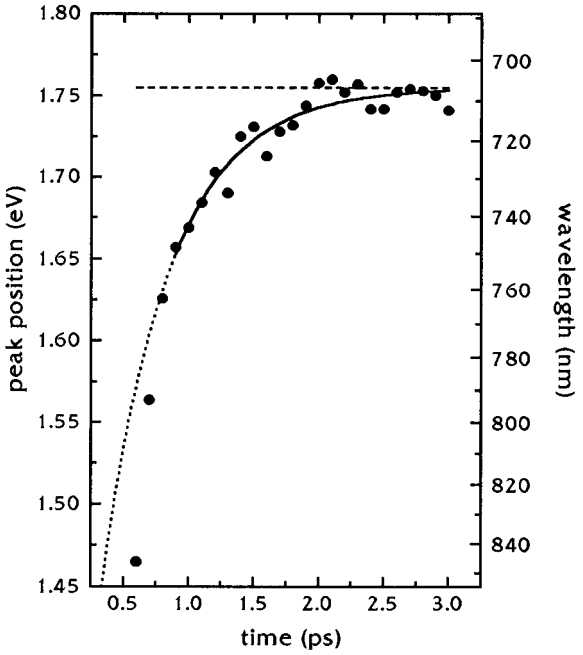

Figure 5. Variation with time of the peak position of the Gaussian−Lorentzian functions that have been used to fit the observed transient spectra in liquid D_2O. The solid line represents an exponential function, with characteristic rise time equal to 0.52 ps, which was fitted through the data points from 0.9 to 3.0 ps. The dotted curve is the extrapolation of this function to shorter time delays. The dashed horizontal line indicates the energy (and wavelength) at which the fully hydrated electron exhibits maximum absorption in D_2O (ref 70).

that slightly exceed the position of the absorption maximum. We excluded most of the low-energy part of the spectrum to focus on the e^-_{sb} itself. For each delay considered, we fitted the observed spectrum with a Gaussian−Lorentzian function which is known to adequately describe the absorption spectrum of e^-_{aq}.[70] Figure 4a shows that the width on the Lorentzian (blue) side does not vary with time and equals, on average, the value that was measured for e^-_{aq} by radiolysis.[70] This crucial observation suggests that the variation in the position of the e^-_{sb} spectrum's maximum is not accompanied by a modification of its shape. In contrast, the width on the Gaussian (red) side decreases with time and tends only slowly toward the value measured for e^-_{aq}. This is most likely due to the fact that the e^-_{wb} (and possibly another longer-lived component, as we shall see in section 4) contributes to the absorption at these wavelengths. It thus appears more reliable to characterize the intensity of the e^-_{sb} signal with the height of the maximum rather than with the total area that would include contributions from other absorbing species. Note that, in view of the constancy of the e^-_{sb} spectral width that we observe on the blue side, the height of the e^-_{sb} spectrum should constitute a good measure of the buildup in the visible that results from the stepwise transition between e^-_{wb} and e^-_{sb}.

Figure 4b shows that the time dependence of the maximum height of the transient spectra can be well fitted, for delays >0.8 ps, with an exponential function of characteristic rise time equal to 0.39 ps. For shorter delays, the contribution of the infrared absorbing species affects too much the amplitude of the maximum to yield results that would reflect the evolution of the e^-_{sb} absorption. Moreover, the effects of the convolution (due to the duration of the pulses) and of the noninstantaneous trapping of the electrons are expected to cause a departure from a simple exponential time dependence at short delays.

Finally, when we study the variation with time of the transient peak position, we find that it also displays a monoexponential behavior when the positions of the absorption maxima are expressed in units of energy. This systematic blue shift of the e^-_{sb} spectrum is shown in Figure 5. A characteristic shifting time of 0.52 ps is obtained when we again exclude delays shorter than 0.9 ps for which the position of the transient peak is likely to be influenced by species other than the e^-_{sb} itself.

In the light of this rather simple analysis of our results, it appears that the process of electron solvation in water involves essentially the same elements that were identified in our study of electron solvation in methanol.[31,36] In fact, we observe a continuous blue shift of the e^-_{sb} spectrum which is concomitant to the well-known stepwise transition. In this case, however, the two processes are harder to separate owing to the comparable time scales over which they take place. In order to see if the hybrid model, which accounted quantitatively for the observed kinetics of electron solvation in methanol, can do as well when the solvent is liquid D_2O, we must perform a simultaneous fit on all the measured kinetic traces. This fit, which would need to incorporate the convolution of the data (a critical aspect when dealing with water), should allow one to circumscribe more precisely various parameters of the hybrid model of solvation such as the various relaxation times involved, the amplitude of the spectral shifts, and the relative importance of the channel through which quasi-free electrons can get trapped directly into e^-_{sb} electron−solvent configurations. It also seems to be the only approach that would allow a characterization of the evasive e^-_{wb} spectrum.

4. Fit of the Kinetics

4.1. The Elements and Constraints of the Model. As mentioned above, the fit of the kinetic traces was done using the hybrid model that we put forth previously to explain the spectral changes associated with the solvation of electrons in methanol.[31,36] In short, this model describes the trapping of electrons into two different *unrelaxed* trapped states, namely e^-_{wb} and e^-_{sb}, and accounts for two types of relaxation mechanisms that can occur concurrently. The first one is a first-order stepwise transition between e^-_{wb} and e^-_{sb} which takes place with a characteristic time τ_{step}. The second one is a continuous blue shift (monoexponential in energy) of the spectra of both species. The model assumes, for simplicity, that the same characteristic time τ_{cont} applies to the shift of e^-_{wb} and e^-_{sb} and that this process starts from the moment the electron gets trapped in either of those states. The extents in energy of the two shifts, ΔE_{wb} and ΔE_{sb}, are allowed to differ from one another. Since the e^-_{sb} is modeled to relax continuously into the fully solvated species, its absorption spectrum is assumed to be identical in amplitude and shape to that of e^-_{aq} but translated as a whole along the energy axis. Jou and Freeman[70] very closely described this e^-_{aq} spectrum by a Gaussian−Lorentzian function. These authors found that, for liquid D_2O at room temperature, the half-widths at half-maximum (hwhm) on the Gaussian (red) and on the Lorentzian (blue) sides are 0.349 and 0.453 eV, respectively, and that the position of the absorption maximum lies at 1.755 eV.[70] Those values being determined from an independent experiment, we kept them fixed in our fit. As for the spectrum of e^-_{wb}, it is simply described (to avoid overparametrizing the problem) as another blue-shifting Gaussian−Lorentzian function whose shape (simply determined by W_G and W_L, the Gaussian and Lorentzian hwhm, respectively) and maximum extinction coefficient ϵ_{max} remain constant during the whole hydration process.[71] Its peak is set to be located at an energy $E_{max}°$ before the beginning of the continuous shift. Trapping is modeled as a first-order process with a characteristic time τ_{trap}. Direct trapping of the quasi-free electrons into the e^-_{sb} configuration is allowed to occur, and its probability is noted P_{dir}. The geminate recombination, which is assumed to start as the electron gets trapped, is also included inside the convolution integral of the combined pulses and applied uniformly over the whole spectral range.

In view of the fact that the powerful pump pulse that we use lies in the visible (around 620 nm), we expect the early-trapped electrons to be promoted to quasi-free states via the absorption of this light pulse. Our numerical simulations of the experiment have shown that this phenomenon causes an apparent delay in the electron-trapping kinetics. It also makes the convolution of the pulses narrower since the time span over which the quasi-free electrons are generated prior to this apparent delay becomes irrelevant. Various fits indicate that the best results are obtained when trapping is set to start 0.15 ± 0.05 ps after the passage of the pump's intensity maximum (time zero).

Concerning the absorption and emission features that appear around time zero, they are accounted for by the addition (outside the convolution integral) of a signal that always has the same kinetic behavior but whose intensity is allowed to vary with the probe wavelength. It should be noted that three types of such transient components are observed. First, an inverse Raman absorption is obtained when the energy difference between the probe and the pump photons corresponds to the energy of a molecular vibrational transition[30] (see Figures 1 and 2a). Second, a stimulated Raman emission is observed when the same energy difference is in favor of the pump photons.[30] For both of those cases, the transient signal can be approximated by a simple Gaussian. Third, we find a supplementary signal that appears very clearly at our lowest probe wavelengths and that gradually blends into the absorbance rise associated with the electron when this wavelength is increased. The presence of characteristic structures in those rises suggests that this component should be included over the whole studied spectral range. Its kinetics, which is directly observable below 600 nm, displays a central maximum at time zero which is preceded and followed by small minima in the absorbance (see Figure 2). This kinetic behavior can be well described by the function $0.123 \exp(-t^2/s_1^2) - 0.089 \exp(-t^2/s_2^2)$, with t in picoseconds and with $s_1 = 0.435$ ps and $s_2 = 0.501$ ps. The intensity of the signal, which varies from one wavelength to another, is accounted for by a multiplicative factor in our fit. This feature is most likely due to nonlinear effects that result from an influence of the high transient electric field of the pump pulse on the water refraction index. Its characteristic kinetic signature and its extension over the whole spectrum investigated indicate that it is not caused by the absorption of a transient chemical species like an ionized or an electronically excited solvent molecule, as was surmised in previous studies.[19,21,26,27,35]

4.2. The Overall Fit. The estimation of these parameters is done with the nonlinear least-squares algorithm of Marquardt which is applied to fit simultaneously the 20 observed kinetic traces. As can be seen in Figures 1 and 2, the fits are very satisfactory at all wavelengths. However, it is important to note that, in order to obtain those good fits, we had to extend our model to add a weak source of absorption in the near infrared (800−1100 nm). In fact, the kinetic traces at those wavelengths display a relatively long-lasting absorbance that was noted in our presentation of Figures 2 and 3, and which appears to be inconsistent with the faster stepwise transition and spectral blue shift that are observed at the other wavelengths. To keep the description of this near-infrared component as simple as possible, we modeled its absorption spectrum with an unshifting Gaussian function. The fit revealed that the characteristic decay time of this component is indeed quite long (2.0 ± 0.2 ps) in comparison to the values of the other temporal fitting parameters of the model, *i.e.*, $\tau_{trap} = 0.16 \pm 0.02$ ps, $\tau_{step} = 0.41 \pm 0.02$ ps, and $\tau_{cont} = 0.51 \pm 0.03$ ps.[72] An important result of the fit is also the determination of the extents ΔE_{wb} and ΔE_{sb} of the blue shifts experienced by the two trapped electron states. Those were found to be 0.06 ± 0.02 and 0.34 ± 0.02 eV, respectively. The probability P_{dir} of direct trapping into the e^-_{sb} configuration was determined at 0.34 ± 0.04. As for the absorption spectrum of e^-_{wb}, it can be characterized with $\epsilon_{max} = 1660 \pm 120$ m^2/mol, $E_{max}° = 0.95 \pm 0.01$ eV, $W_G = 0.11 \pm 0.01$ eV, and $W_L = 0.15 \pm 0.02$ eV. Figure 6 shows how this spectrum compares with that of e^-_{sb} and of the near-infrared component. One can see that the amplitude of the e^-_{wb} spectrum is comparable to that of e^-_{sb}, its small apparent contribution in Figure 3 being attributable to the fact that (i) its lifetime τ_{step} is not much longer than its formation time τ_{trap} and (ii) a nonnegligible proportion P_{dir} of the electrons do not transit through this state. Finally, concerning the absorbance structures that are observed around time zero and attributed to nonlinear effects caused by the intense pump pulse, we find that the amplitude of these structures (once normalized like the rest of the kinetics) decreases slightly with probe wavelength. For all practical purposes, they can essentially be considered as constant over the studied spectral range. The main peak at time zero reaches, on average, a value of 0.05 in absorbance.

We find it important to note at this point that the determination of the fitting parameters and of their uncertainty is done in the context of a fit for which some constraints were imposed,

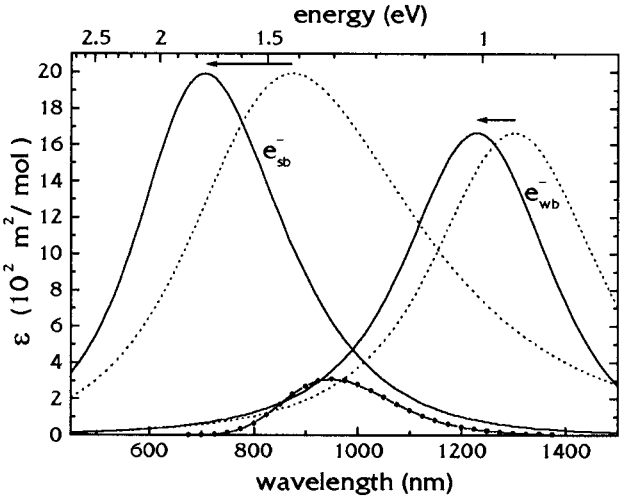

Figure 6. Molar extinction coefficients ϵ (SI units are used: 1 m^2/mol = 10 M^{-1} cm^{-1}) of the various species that are included in the fit of the observed kinetics. The dotted lines represent the spectra of e^-_{wb} and e^-_{sb} before any continuous shift has occurred. The solid lines represent the spectra in the long-time limit, *i.e.*, when the continuous shift is completed. The arrows indicate the amplitude of the blue shifts. One should note that, on the energy scale, the widths of the spectra remain constant. The absorption coefficient of the near-infrared component (−●−) is calculated here with the assumption that every ionization of a water molecule leads to the formation of this component.

often on the basis of direct experimental measurements. Those constraints include the temporal width of the pump−probe convolution, the normalization of the various kinetic traces, the positions of time zero, and the delay imposed upon electron trapping which results from the absorption of the pump pulse by early-trapped electrons. Changes in any of those constraints obviously affect the determination of the fitting parameters. We found in particular that the characteristic times τ_{trap} , τ_{step} , and τ_{cont} are correlated to the electron-trapping delay mentioned above. One should thus consider that the uncertainties given here constitute minimal values of the 95% confidence intervals. It is interesting to note that all our trial fits resulted in a value of τ_{cont} that exceeded that of τ_{step} by about 0.1 ps.

5. Discussion

5.1. General Considerations. If we compare the results of our empirical analysis of the transient spectra (see Figures 3−5) to those of the more rigorous overall fit on the 20 kinetic traces, we find that the main features of the hydration kinetics seem to have been essentially grasped by the former approach. In fact, the fit, which includes many specific aspects of the experiment, confirms that our entire set of kinetic traces can be well described with the hybrid model that involves a stepwise transition as well as a monoexponential continuous spectral blue shift. The characteristic times of the stepwise transition (∼0.4 ps) and of the e^-_{sb} shift (∼0.5 ps) could be well estimated from the transient spectra. This is also true for the extent in energy (0.3−0.4 eV) of the continuous blue shift. Moreover, the fit confirms the presence of a long-lasting absorption component in the near infrared (between 800 and 1100 nm). As for the spectrum of the e^-_{wb} species, its maximum absorption around 1300 nm (see Figure 6) could already be estimated from an inspection of the transient spectra of Figure 3. However, the fit proved essential in the determination of the formation time of this species (between 100 and 200 fs) and in the assessment of its rather small spectral blue shift. Finally, the existence and importance of a direct channel that allows the quasi-free electrons to avoid transiting through the intermediate e^-_{wb} state could only be evidenced by means of the complete fitting procedure.

It is interesting at this point to recall the results that were obtained in a similar analysis of the electron solvation kinetics in ambient temperature methanol.[31,36] In that case, the characteristic relaxation times were much larger, owing to the slower molecular motions in this liquid, but the same kinds of phenomena were observed. Even from a quantitative point of view, it is worth noting that the extent of the e^-_{sb} spectral blue shift was essentially the same as that obtained in the present study. As for the probability P_{dir} of direct trapping into the e^-_{sb} state, it was also found to exist in methanol; its value was somewhat larger in that medium than it appears to be in D_2O (0.54 in comparison to 0.34). The similarity between the mechanisms of electron solvation in those two polar media has often been surmised and is, to a certain extent, informative. For example, it could be argued that the observation of a continuous blue shift of the e^-_{sb} spectrum originates mainly from a rapid cooling of the solvated electrons' immediate surroundings.[28] However, this hypothesis does not hold in view of the fact that the characteristic time of the spectral shift correlates with the time of a molecular rotation in the studied liquid[5,10,12,18,29,34] (*e.g.*, it is more than 20 times slower in methanol[31,36] than in water) and not with the coefficient of thermal diffusivity[3] which is about the same in methanol and in water.[73]

5.2. The Electron Trapping and the Stepwise Transition. Comparing the present determination of τ_{trap} and τ_{step} to those of the previous studies of electron hydration brings us into the heart of some controversies that still prevail in this field. In fact, there is a rather strong dispersion in the quantitative assessment of those two relaxation times. Reviewing the literature on this issue for the case of H_2O, we find the values τ_{trap} = 110 fs, τ_{step} = 240 fs (ref 14); τ_{trap} = 180 fs, τ_{step} = 540 fs (ref 19); $\tau_{trap} + \tau_{step}$ = 650 fs (ref 26); τ_{step} = 310 fs (ref 28); τ_{trap} = 150 fs, τ_{step} = 500 fs (ref 32); τ_{trap} = 300 fs, τ_{step} = 540 fs (ref 37); τ_{trap} = 180 fs, τ_{step} = 540 fs (ref 38). Theoretical studies based on classical molecular dynamics simulations of the solvent coupled with quantum adiabatic and nonadiabatic simulations of the electron's wave function also yielded various values of those times, such as: τ_{trap} ∼30 fs (ref 46); τ_{step} ∼1000 fs (ref 50); τ_{step} = 220 fs (ref 51); τ_{step} = 160 fs (ref 53). Finally, we can also quote the work of Keszei *et al.*[56] who reanalyzed the experimental data of Migus *et al.*[14] and the simulation results of Murphrey and Rossky[53] to find that the former could lead to τ_{trap} = 100 fs and τ_{step} = 330 fs, whereas the latter can be fitted with τ_{trap} = 92 fs and τ_{step} = 67 fs. The dispersion of those results reveals the absence of consensus on a quantitative determination of those kinetic parameters. The general trend that can be retained is that τ_{trap} seems to be less than 300 fs and that τ_{step} exceeds τ_{trap} by a few hundred femtoseconds.

If we consider the case of electron hydration in D_2O, we note that much fewer studies have been performed. In each of them it was found that the characteristic times were slightly larger in D_2O. Long *et al.*[17] suggested that the difference is ∼30%, whereas Gauduel *et al.*[21,23,27] estimated it to be even smaller (∼5−10%). A recent quantum nonadiabatic simulation study[59] also led the authors to conclude that the isotope effect should be small enough to be difficult to observe. This result contrasted sharply with an earlier simulation study[51] which yielded a value of τ_{step} in D_2O (800 fs) that largely exceeded its calculated counterpart in H_2O (200 fs). In view of all this, the values τ_{trap} = 160 fs and τ_{step} = 410 fs that we obtain for the hydration kinetics in D_2O can be considered to fall well within the range of previous determinations.

We wish to point out here the similarity between the electron-trapping time which is generally found in water (~150 fs) and the one that we obtained in our study of electron solvation in methanol (330 fs).[31,36] On a physical basis, one expects τ_{trap} to be of the same order in those media since the trapping time should be more related to the density of preexisting traps than to the characteristic rotation time of the solvent molecules. In contrast, the stepwise transition time is found to be more than 10 times longer in methanol[10,12,18,29,31,35,36] than in water. The only study in which τ_{step} is considered to be essentially the same in water and in various alcohols is that of Walhout *et al.*[34]

5.3. The Direct Channel of Deep Trapping. If we turn to the determination of P_{dir}, we find that most studies have either not considered this possibility or assumed it to be negligible. Those who tried to estimate it found $P_{dir} = 0.2$ (ref 48), 0.5 (ref 50), 0.6 (ref 53), 0.22 or 0.66 (ref 56), and <0.5 (ref 37). These values (including our own: $P_{dir} = 0.34$) fall into a range (0.2−0.7) which constitutes a reasonable consensus. We should point out, however, that the existence of this direct deep-trapping channel in water is not firmly established on an experimental basis since all the measured hydration kinetics can be fitted quite satisfactorily without including such a parameter. This is not the case for the solvation of electrons in alcohols of various chain lengths for which a subpicosecond growth of the absorption in the visible has often been observed.[12,13,26,31,36] The basis for including the P_{dir} parameter in our modeling of electron hydration thus rests mainly on the analogy that we are tempted to draw between water and the alcohols. Finally, we wish to point out here that the physical meaning of our parameter P_{dir} differs from that of other authors who consider that once the electron has gone through this channel, its solvation is completed.[37,48,54,56] In our model, the solvation only ends when the continuous blue shift of the e^-_{sb} spectrum has finished.

5.4. The Continuous Relaxation. From a physical point of view, the solvation of a charged entity in a polar molecular medium requires some reorientation and displacement of the surrounding molecules. As a consequence, the existence of spectral shifts of the absorbing species is almost certain. The main question that remains is to know whether or not these shifts can be observed experimentally. They could, for example, be too small (in energy) or too fast to be detected. The fact is that those shifts *are* observed during the solvation of molecular ions and dipoles in various liquids (including water).[74−79] In the case of electron solvation in alcohols, earlier studies at low temperature[3,4,6−9] and more recent ones at room temperature[18,29,31,34,36,39] have shown that the role played by the continuous relaxation of the solvent in the spectral kinetics cannot be neglected in these media. In spite of this, it has generally been left out in the modeling of electron hydration, the rationale for this being that a great deal of the observed spectral changes seems to be accounted for by the sole transition between e^-_{wb} and e^-_{sb}.[14,19] Messmer and Simon[48] were the first to include this element in their analysis of the measured[14] transient electron absorption spectra in liquid water. They introduced a very extended blue shift (~1.2 eV) that only applied to a fraction of the electrons and whose characteristic time was 250 fs. Barbara and co-workers[28] also found it necessary to invoke such a blue shift in their modeling of a fairly different experiment in which they performed a 1.6-eV excitation on a population of fully relaxed hydrated electrons. They observed complicated kinetic responses in the near infrared and attributed them to the occurrence of a continuous blue shift that had a small amplitude (~0.1 eV) and which was rather slow (~1.2 ps). Considering that this relaxation process took place after the electrons have returned to the strongly bound state, they named it "ground-state solvation". The small extent in energy of the blue shift observed in these experiments may be attributed to the fact that the electrons start from a fully relaxed state. The same measurements were later reanalyzed through a comparison with quantum nonadiabatic simulations,[55,57] and it was suggested that the observed kinetics were mainly due to a continuous relaxation (with characteristic time 240 fs) of the solvent around the intermediate e^-_{wb} state rather than around the final e^-_{sb} state.

It should be pointed out here that all the molecular dynamics simulations of electron hydration displayed a continuous relaxation of the available electronic states both before and after the passage of the electron from one state to another. In the case where the electrons were considered to start out from a quasi-free state, the kinetics of this continuous relaxation was universally found to consist of a fast (<50 fs) component and a slower (~200 fs) one.[46,47,53] This latter component of τ_{cont} is essentially equal to the longitudinal dielectric relaxation time of liquid water which, according to the continuum dielectric models, should govern the solvent response to the emergence of a point charge.[44,76,80]

In the present study, we find that the continuous solvent response, although not rate-limiting as such ($\tau_{cont} = 510$ fs > $\tau_{step} = 410$ fs), plays a significant role in the observed spectral kinetics that result from the hydration of electrons in D_2O. We also find that its simple description with a monoexponential function suffices to grasp its main contribution. It should be noted that in water, in contrast to the results of our analysis of electron solvation in methanol,[31,36] the extent in energy of the e^-_{wb} blue shift is essentially negligible ($\Delta E_{wb} = 0.06$ eV). That of the e^-_{sb} species ($\Delta E_{sb} = 0.34$ eV), however, is considerable. In earlier studies,[8,18,29,31] this blue shift was attributed to the "long-range" contribution to the solvation energy, which is expected to build up continuously due to the involvement of a large number of molecular positions and orientations. At this point, the actual contribution of the polarization to the solvation energy remains uncertain. On one hand, observations of the solvation of electrons in dilute mixtures of alcohols in alkanes[81] suggest that only a few molecules of alcohols seem to be needed to provide a deep trap for the electrons. On the other hand, the attachment of electrons to water clusters of various sizes[82−84] indicate that the electron binding is sensitive to a rather extended environment. A "long-range" contribution of a few tenths of an electronvolt would not be at odds with these latter studies.

5.5. The Excess Absorption in the Near Infrared. Another aspect of the observed spectral kinetics is the existence of a long-lasting absorption in the region 900−1100 nm that we denote here as the near infrared. As was pointed out in section 3, this excess absorption can readily be observed in the kinetic traces as well as in the transient spectra. Our overall fit revealed that it could be accounted for by including a supplementary absorbing component which appears within a few hundred femtoseconds and decays with a time constant as large as 2 ps. In view of the spectral location of this component, it is natural to draw a parallel between our observations and those of Gauduel and co-workers.[20,24,27] Those authors first identified very clearly, in highly concentrated HCl aqueous solutions, an absorbing "species" whose spectrum (probed at many wavelengths) peaked around 920 nm and which decayed with a fairly long characteristic time of 850 fs.[20] They associated this absorption to a transient [H_3O^+ : e^-] pair which is likely to form at the time of electron trapping in such highly acidic solutions. Subsequently, they considered the existence of this kind of "encounter pairs"[85] in pure liquid water and attributed

to them the excess absorption that they observed at 820 nm.[24,27,86] The case was not very convincing in H_2O since the kinetic parameters associated with the formation and decay of this species were not significantly different from those of e^-_{wb} (as determined by these authors).[24] In D_2O, however, the excess absorption had a distinctive kinetic behavior: its decay time (0.77 ps) was longer than the τ_{step} of 0.25 ps derived in that study.[27] It is worth noting here that a recent study[38] of electron hydration in H_2O also mentions the observation of "an additional short-lived ($\tau \sim 1$ ps) infrared-absorbing kinetic component" at 750 nm but does not give further details.

We find that if we attempt to fit our measured kinetic traces in D_2O *without* including a continuous blue shift of the trapped electrons' spectra, we are also led to resort to the introduction of a strongly[87] absorbing component in the near infrared which decays with a characteristic time of 0.87 ps. The fit is then fairly good but fails to account satisfactorily for the rise of the absorption on the blue side of the e^-_{sb} spectrum and for the long-time component of the excess absorption around 950 nm. Nevertheless, it is important to realize that the presence of a supplementary species conveniently located in the near infrared causes spectral changes that are not readily distinguishable from a spectral blue shift of e^-_{sb}.[86] We find that, in order to discriminate between those two possibilities, one has to consider simultaneously a number of kinetic traces that cover a wide range of probing wavelengths. It is therefore possible that the departure from a strictly two-state kinetics that Gauduel and co-workers[24,27] observed in the near infrared (at 820 nm) was due to the presence of a continuous blue shift that they did not account for. All one can say is that they probed an intermediate spectral region where the relaxation kinetics was slower than that measured in the visible and further in the infrared. The same observation was made by Chase and Hunt[3] in the alcohols and led them to conclude that it was "probably due to complex spectral shifts" that accompany the solvation. A thorough discussion on the interpretation of slower kinetics at intermediate wavelengths can also be found in ref 7.

The approach adopted by Gauduel and co-workers,[24,27] which consisted of analyzing separately the kinetics at a few test wavelengths, led them to introduce a supplementary absorbing species in quite an *ad hoc* fashion. The best justification for their choice remains the qualitative analogy that could be drawn between this phenomenon and the spectrally well-characterized species that they identified in aqueous solutions containing 11 M of HCl.

Similarly, we can ask ourselves whether or not the small[87] supplementary absorbing component that we introduced in our model simply constitutes a manifestation of our inability to fully describe a more global relaxation feature. Attempts have been made, for example, to model the continuous shift with a more complex solvent response function than a monoexponential. So far, none of those were as successful as the overall fit that we present here. For now, we consider the physical origin of the long-lasting absorption in the near infrared as an open question.

5.6. The Existence of an Isosbestic Wavelength. Regarding the kinetics in the near infrared, we wish to comment on the much controversial notion of isosbestic wavelength which is predicted by a description of the hydration that rests strictly on a stepwise transition between e^-_{wb} and e^-_{sb}.[14,19,24,37,48] Most of the debate on this issue refers to the results obtained in H_2O, but the same reasoning also applies to the case of D_2O. Even though there is always a wavelength at which the extinction coefficients of e^-_{wb} and e^-_{sb} are equal, it does not necessarily lead to the presence of an isosbestic point in the transient spectra. In the framework of the hybrid model that we promote, the spectra of the absorbing species shift with time and thus no such point should be observed. As pointed out in a previous study,[24] it is also essential to carefully correct for the geminate recombination kinetics before looking for a probe wavelength that would exhibit a flat hydration kinetics. As well, one should consider the possibility that a supplementary absorbing component contributes to the signal[24] and that the reactivity of the e^-_{wb}[49] could cause the total number of trapped electrons to decrease in the course of solvation. In our case, we found that none of our 20 kinetic traces showed the behavior of an isosbestic wavelength. The original observation of Long *et al.*[19] of such a behavior at 820 nm in H_2O was contested by Pommeret *et al.*[24] who measured, at this very position, a decay that could not be solely attributed to their description of the geminate recombination. These latter authors did not find any probe wavelength for which the kinetic trace (once corrected for the recombination) could be fitted to a single time constant. This observation confirmed the fact that no isosbestic point appeared in their transient spectra.[14]

The absence of an isosbestic wavelength was also quite clearly evidenced by the results of recent experiments[28] that were designed to monitor the excitation of e^-_{sb} into e^-_{wb} and its subsequent stepwise deexcitation. In the case where only those two species absorb and where there are no continuous shifts of the spectra, one would have expected the isosbestic wavelength to manifest itself with an absence of variation in the absorbance during the whole process. In contrast, complicated transient behaviors were observed in the range 750−900 nm, and it was concluded that continuous spectral shifts are involved in the relaxation of the system.[28,55,57] In spite of this, Shi *et al.*[37] recently based again their analysis of the hydration kinetics on the existence of an isosbestic wavelength at 820 nm. A careful analysis of the contribution of their early recombination kinetics and a display of their transient absorption spectra would perhaps help in elucidating this apparent contradiction between different sets of experimental results.

5.7. The Events Preceding Electron Trapping. We end this discussion with some considerations on the energetics of water photoionization and on the possible absorption of light by quasi-free electrons. As already mentioned in section 2, our experiment is based on the ionizing properties of an intense 620-nm (2-eV) light pulse. It thus differs from the other experimental setups that make use of more energetic photons to generate the excess electrons.[14,19,26,32,38,68] Various studies have suggested that the process of ionization of the solvent molecules conditions the state from which the electrons begin to interact with the medium as isolated charges.[22,25,32,38,67,68,88,89] As a consequence, different ionization processes can be distinguished from an analysis of the recombination kinetics that follows hydration.[68] Upon examining our electron survival function that was given in section 3 and displayed in Figure 1, one finds that 22% of the electrons have undergone a geminate recombination 70 ps after their generation in the medium. This proportion corresponds to that found when two 5-eV photons are used to ionize water.[26,68] In the case where only 8 eV are deposited, the recombination is significantly more important.[15−17,27,68] In contrast, an ionization that involves the deposition of 12 eV or more results in a recombination kinetics that is extremely weak and slow.[32,68] It thus appears quite clearly that five 2-eV photons are needed to produce the ionizations that we observe.

As for the intermediate states that intervene in the multiphoton ionization, they cannot be unambiguously determined. Our earlier studies[25,30] of the variation of the e^-_{aq} absorbance with laser irradiance raised the question of the role that could be

played by an excited state of the water molecules. One can also wonder whether or not the ionization proceeds through the absorption of 8 eV (four photons) in a first stage which would be followed by electron trapping and subsequent detrapping via the absorption of a fifth photon. In fact, we already mentioned that our observed hydration kinetics are consistent with a delay that could be caused by the absorption of the pump pulse photons by trapped electrons.

The subsequent absorption of light by the initially created quasi-free electrons remains controversial. The fact that our recombination kinetics is significantly faster than that of experiments where 12 eV are used to ionize indicates that the quasi-free electrons do not absorb supplementary 2-eV photons from our pump pulse. It has been suggested[53,56] that they may absorb quite strongly in the near infrared and even in the visible (ϵ at maximum $\sim 2 \times 10^3$ m^2/mol), and some modelings of the kinetics have included this feature.[56] Since this property of quasi-free electrons is quite uncertain,[90] we preferred not to introduce it in our model. Given the short time of localization of the electrons, the spectral characteristics of the quasi-free states are very difficult to assess experimentally and cannot realistically be extracted from our type of pump−probe experiment.

6. Conclusion

In conclusion, we wish to recall that the present study, performed over a wide spectral range and with a large number (20) of probing wavelengths, was designed to grasp as globally as possible the spectral changes that accompany the hydration of electrons. It was found from an inspection of the transient absorption spectra that the well-known stepwise transition between the weakly bound (e^-_{wb}) and strongly bound (e^-_{sb}) electron−solvent configurations is accompanied by a slightly slower continuous blue shift of the latter species' spectrum. An examination of the time dependence of the height and position in energy of the absorption maximum reveals that both the absorption buildup and the shift can be adequately modeled with monoexponential functions. Moreover, we find that the evolution of the e^-_{sb} electron−solvent configuration is not accompanied by complicated modifications of its spectral shape.

To put those observations to the test of a more rigorous quantitative modeling of the measured kinetics, we performed various overall fits on our 20 kinetic traces. We found that our hybrid model, which was developed to account for electron solvation in methanol, was also able to describe accurately the spectral manifestations of electron hydration. The fit confirmed the results of our preliminary analysis of the transient spectra, yielding characteristic relaxation times of 0.41 ± 0.02 and 0.51 ± 0.03 ps for the stepwise transition and the continuous blue shift, respectively. It also allowed a quantitative determination of the characteristic electron-trapping time (0.16 ± 0.02 ps) and of the probability (0.34 ± 0.04) of direct trapping into the e^-_{sb} state. These values fall well within the range of those that can be found in the literature. The extent in energy of the e^-_{sb} blue shift (0.34 ± 0.02 eV) is very similar to the one that was found to apply to the case of electron solvation in methanol.[31,36] The fit could also be used to characterize the absorption spectrum of the evasive e^-_{wb} species which extends very little in the visible and displays a maximum around 1250 nm. The blue shift of the e^-_{wb} spectrum was found to be small.

The departure that we observe from the predictions of the so-called two-state model of electron solvation (involving only the stepwise transition) is not new. Several electron solvation studies in alcohols have revealed the existence of continuous shifts of the absorption spectra.[3,4,6−9,18,29,31,36,39] In water, however, the two-state model is still often considered as the standard one even though it was shown to be unable to account for the slower kinetics observed in the near infrared. Some authors have evoked the existence of a supplementary absorbing species to explain this.[24,27,38] Others have concluded that the spectral shifts resulting from the relaxation of the medium play an important role in the near infrared kinetics.[28,48] The present study strongly supports the latter approach. We found that resorting solely to a supplementary component does not allow to fit globally all the observed kinetics as well as when a continuous spectral shift is introduced. More importantly, the hypothesis of the continuous spectral shift relies on sound physical considerations regarding the expected relaxation of the solvent as a whole. In that sense, it appears as a more natural approach to interpret the experimental results. The simplicity of our description of the shift (with a monoexponential variation with time) and its similarity with those established for electron solvation in alcohols and for ion or dipole solvation in polar media in general also reinforce the model we have adopted. We must say, however, that we did introduce in our fit a small supplementary absorbing component in the near infrared to account for the slow (∼2 ps) relaxation which is observed around 950 nm. The physical origin of this long-lasting absorption remains an open question.

In the present study, we insisted on the necessity of examining simultaneously a large number of probe wavelengths on a wide spectral range to capture a global picture of the relaxation phenomena involved. We also showed that it is crucial to account for the slower kinetic features, such as the geminate recombination and the excess of absorption in the near infrared, which are entangled to the hydration kinetics at shorter times. Bearing this in mind, the best way to further elucidate this subject is to improve the time resolution of the measurements, which is not yet significantly better than the characteristic times of the observed phenomena in water.

Acknowledgment. Funding for this research was provided by the Medical Research Council of Canada. This support is herewith gratefully acknowledged.

References and Notes

(1) Rentzepis, P. M.; Jones, R. P.; Jortner, J. *J. Chem. Phys.* **1973**, *59*, 766.
(2) Baxendale, J. H.; Wardman, P. *J. Chem. Soc., Faraday Trans. 1* **1973**, *69*, 584.
(3) Chase, W. J.; Hunt, J. W. *J. Phys. Chem.* **1975**, *79*, 2835.
(4) Klassen, N. V.; Gillis, H. A.; Teather, G. G.; Kevan, L. *J. Chem. Phys.* **1975**, *62*, 2474.
(5) Kenney-Wallace, G. A.; Jonah, C. D. *Chem. Phys. Lett.* **1976**, *39*, 596.
(6) Baxendale, J. H.; Sharpe, P. H. G. *Int. J. Radiat. Phys. Chem.* **1976**, *8*, 621.
(7) Gilles, L.; Bono, M. R.; Schmidt, M. *Can. J. Chem.* **1977**, *55*, 2003.
(8) Okazaki, K.; Freeman, G. R. *Can. J. Chem.* **1978**, *56*, 2305.
(9) Ogasawara, M.; Shimizu, K.; Yoshida, K.; Kroh, J.; Yoshida, H. *Chem. Phys. Lett.* **1979**, *64*, 43. Ogasawara, M.; Shimizu, K.; Yoshida, H. *Radiat. Phys. Chem.* **1981**, *17*, 331.
(10) Wang, Y.; Crawford, M. K.; McAuliffe, M. J.; Eisenthal, K. B. *Chem. Phys. Lett.* **1980**, *74*, 160.
(11) Wiesenfeld, J. M.; Ippen, E. P. *Chem. Phys. Lett.* **1980**, *73*, 47.
(12) Kenney-Wallace, G. A.; Jonah, C. D. *J. Phys. Chem.* **1982**, *86*, 2572.
(13) Lewis, M. A.; Jonah, C. D. *J. Phys. Chem.* **1986**, *90*, 5367.
(14) Migus, A.; Gauduel, Y.; Martin, J. L.; Antonetti, A. *Phys. Rev. Lett.* **1987**, *58*, 1559.
(15) Lu, H.; Long, F. H.; Bowman, R. M.; Eisenthal, K. B. *J. Phys. Chem.* **1989**, *93*, 27.
(16) Gauduel, Y.; Pommeret, S.; Migus, A.; Antonetti, A. *J. Phys. Chem.* **1989**, *93*, 3880.
(17) Long, F. H.; Lu, H.; Eisenthal, K. B. *Chem. Phys. Lett.* **1989**, *160*, 464. Lu, H.; Long, F. H.; Eisenthal, K. B. *J. Opt. Soc. Am. B* **1990**, *7*, 1511.

(18) Hirata, Y.; Murata, N.; Tanioka, Y.; Mataga, N. *J. Phys. Chem.* **1989**, *93*, 4527. Hirata,Y.; Mataga, N. *J. Phys. Chem.* **1990**, *94*, 8503; **1991**, *95*, 9067.
(19) Long, F. H.; Lu, H.; Eisenthal, K. B. *Phys. Rev. Lett.* **1990**, *64*, 1469.
(20) Gauduel, Y.; Pommeret, S.; Migus, A.; Yamada, N.; Antonetti, A. *J. Am. Chem. Soc.* **1990**, *112*, 2925.
(21) Gauduel, Y.; Pommeret, S.; Migus, A.; Antonetti, A. *Chem. Phys.* **1990**, *149*, 1.
(22) Long, F. H.; Lu, H.; Shi, X.; Eisenthal, K. B. *Chem. Phys. Lett.* **1991**, *185*, 47.
(23) Gauduel, Y.; Pommeret, S.; Migus, A.; Antonetti, A. *J. Phys. Chem.* **1991**, *95*, 533.
(24) Pommeret, S.; Antonetti, A.; Gauduel, Y. *J. Am. Chem. Soc.* **1991**, *113*, 9105.
(25) Pépin, C.; Houde, D.; Remita, H.; Goulet, T.; Jay-Gerin, J.-P. *Phys. Rev. Lett.* **1992**, *69*, 3389.
(26) Sander, M.; Brummund, U.; Luther, K.; Troe, J. *Ber. Bunsen-Ges. Phys. Chem.* **1992**, *96*, 1486.
(27) Gauduel, Y.; Pommeret, S.; Antonetti, A. *J. Phys. Chem.* **1993**, *97*, 134.
(28) Alfano, J. C.; Walhout, P. K.; Kimura, Y.; Barbara, P. F. *J. Chem. Phys.* **1993**, *98*, 5996. Kimura, Y.; Alfano, J. C.; Walhout, P. K.; Barbara, P. F. *J. Phys. Chem.* **1994**, *98*, 3450.
(29) Hirata, Y.; Mataga, N. *Prog. React. Kinet.* **1993**, *18*, 273.
(30) Pépin, C.; Houde, D.; Remita, H.; Goulet, T.; Jay-Gerin, J.-P. *J. Chim. Phys.* **1993**, *90*, 745. Houde, D.; Pépin, C.; Goulet, T.; Jay-Gerin, J.-P. In *Mode-Locked and Solid State Lasers, Amplifiers, and Applications*; Piché, M., Pace, P. W., Eds.; Proceedings of SPIE 2041; International Society for Optical Engineering: Bellingham, WA, 1993; pp 139−152.
(31) Pépin, C.; Goulet, T.; Houde, D.; Jay-Gerin, J.-P. *J. Phys. Chem.* **1994**, *98*, 7009.
(32) McGowen, J. L.; Ajo, H. M.; Zhang, J. Z.; Schwartz, B. J. *Chem. Phys. Lett.* **1994**, *231*, 504.
(33) Gauduel, Y. In *Ultrafast Dynamics of Chemical Systems*; Simon, J. D., Ed.; Kluwer Academic: Dordrecht, 1994; pp 81−136 and references therein.
(34) Walhout, P. K.; Alfano, J. C.; Kimura, Y.; Silva, C.; Reid, P. J.; Barbara, P. F. *Chem. Phys. Lett.* **1995**, *232*, 135.
(35) Shi, X.; Long, F. H.; Lu, H.; Eisenthal, K. B. *J. Phys. Chem.* **1995**, *99*, 6917.
(36) Pépin, C.; Goulet, T.; Houde, D.; Jay-Gerin, J.-P. *J. Chim. Phys.* **1996**, *93*, 182.
(37) Shi, X.; Long, F. H.; Lu, H.; Eisenthal, K. B. *J. Phys. Chem.* **1996**, *100*, 11903.
(38) Reuther, A.; Laubereau, A.; Nikogosyan, D. N. *J. Phys. Chem.* **1996**, *100*, 16794.
(39) Zhang, X.; Jonah, C. D. *Chem. Phys. Lett.* **1996**, *262*, 649.
(40) Jortner, J. *Radiat. Res. Suppl.* **1964**, *4*, 24.
(41) Copeland, D. A.; Kestner, N. R.; Jortner, J. *J. Chem. Phys.* **1970**, *53*, 1189.
(42) Webster, B. *J. Phys. Chem.* **1975**, *79*, 2809.
(43) Schnitker, J.; Rossky, P. J.; Kenney-Wallace, G. A. *J. Chem. Phys.* **1986**, *85*, 2986.
(44) Rips, I.; Klafter, J.; Jortner, J. *J. Chem. Phys.* **1988**, *88*, 3246; *89*, 4288.
(45) Motakabbir, K. A.; Rossky, P. J. *Chem. Phys.* **1989**, *129*, 253. Motakabbir, K. A.; Schnitker, J.; Rossky, P. J. *J. Chem. Phys.* **1992**, *97*, 2055.
(46) Rossky, P. J.; Schnitker, J. *J. Phys. Chem.* **1988**, *92*, 4277.
(47) Barnett, R. N.; Landman, U.; Nitzan, A. *J. Chem. Phys.* **1989**, *90*, 4413.
(48) Messmer, M. C.; Simon, J. D. *J. Phys. Chem.* **1990**, *94*, 1220.
(49) Ferradini, C.; Jay-Gerin, J.-P. *Chem. Phys. Lett.* **1990**, *167*, 371.
(50) Webster, F. J.; Schnitker, J.; Friedrichs, M. S.; Friesner, R. A.; Rossky, P. J. *Phys. Rev. Lett.* **1991**, *66*, 3172.
(51) Neria, E.; Nitzan, A.; Barnett, R. N.; Landman, U. *Phys. Rev. Lett.* **1991**, *67*, 1011. Neria, E.; Nitzan, A. *J. Chem. Phys.* **1993**, *99*, 1109.
(52) Jay-Gerin, J.-P.; Ferradini, C. *Can. J. Chem.* **1992**, *70*, 1869. Keszei, E.; Jay-Gerin, J.-P. *Can. J. Chem.* **1992**, *70*, 21.
(53) Murphrey, T. H.; Rossky, P. J. *J. Chem. Phys.* **1993**, *99*, 515.
(54) Keszei, E.; Nagy, S.; Murphrey, T. H.; Rossky, P. J. *J. Chem. Phys.* **1993**, *99*, 2004.
(55) Schwartz, B. J.; Rossky, P. J. *J. Phys. Chem.* **1994**, *98*, 4489. *J. Chem. Phys.* **1994**, *101*, 6902, 6917.
(56) Keszei, E.; Murphrey, T. H.; Rossky, P. J. *J. Phys. Chem.* **1995**, *99*, 22.
(57) Staib, A.; Borgis, D. *J. Chem. Phys.* **1995**, *103*, 2642.
(58) Schwartz, B. J.; Rossky, P. J. *J. Phys Chem.* **1995**, *99*, 2953.
(59) Schwartz, B. J.; Rossky, P. J. *J. Chem. Phys.* **1996**, *105*, 6997.
(60) Bratos, S.; Leicknam, J.-Cl. *Chem. Phys. Lett.* **1996**, *261*, 117.
(61) Prezhdo, O. V.; Rossky, P. J. *J. Phys. Chem.* **1996**, *100*, 17094.
(62) Houée-Levin, C.; Jay-Gerin, J.-P. *J. Phys. Chem.* **1988**, *92*, 6454. Houée-Levin, C.; Tannous, C.; Jay-Gerin, J.-P. *J. Phys. Chem.* **1989**, *93*, 7074.
(63) Mozumder, A. *Radiat. Phys. Chem.* **1988**, *32*, 287.
(64) Hilczer, M.; Tachiya, M. *J. Phys. Chem.* **1996**, *100*, 7691.
(65) Goulet, T.; Jay-Gerin, J.-P. *J. Chem. Phys.* **1992**, *96*, 5076.
(66) Goulet, T.; Mattéi, I.; Jay-Gerin, J.-P. *Can. J. Phys.* **1990**, *68*, 912.
(67) Sander, M. U.; Luther, K.; Troe, J. *Ber. Bunsen-Ges. Phys. Chem.* **1993**, *97*, 953; *J. Phys. Chem.* **1993**, *97*, 11489.
(68) Crowell, R. A.; Bartels, D. M. *J. Phys. Chem.* **1996**, *100*, 17713, 17940.
(69) Pimblott, S. M. *J. Phys. Chem.* **1991**, *95*, 6946.
(70) Jou, F.-Y.; Freeman, G. R. *J. Phys. Chem.* **1979,** *83*, 2383.
(71) The Gaussian−Lorentzian function used to describe the spectrum of e^-_{wb} is the same as that used in ref 70 to fit the spectrum of e^-_{aq}, *i.e.*,

$$f_G(E) = \exp[-\ln(2)\,(E - E_{max})^2/W_G^{\,2}] \text{ and } f_L(E) = [1 + (E - E_{max})^2/W_L^{\,2}]^{-1}$$

(72) Throughout this paper, the uncertainties that we give represent the 95% confidence intervals.
(73) As reviewed in ref 3, the characteristic time for the local cooling of a region that has been heated is related to the inverse of the thermal diffusivity D. Using the relation $D = K\rho^{-1}C_v^{-1}$, where K is the thermal conductivity, ρ the density, and C_v the specific heat, one finds that the values of D in methanol and deuterated water differ by only 20%.
(74) Maroncelli, M.; Fleming, G. R. *J. Chem. Phys.* **1987**, *86*, 6221.
(75) Jarzęba, W.; Walker, G. C.; Johnson, A. E.; Kahlow, M. A.; Barbara, P. F. *J. Phys. Chem.* **1988**, *92*, 7039.
(76) Bagchi, B.; Chandra, A. *Chem. Phys. Lett.* **1989**, *155*, 533.
(77) Weaver, M. J.; McManis, G. E.; Jarzęba, W.; Barbara, P. F. *J. Phys. Chem.* **1990**, *94*, 1715.
(78) Walker, G. C.; Jarzęba, W.; Kang, T. J.; Johnson, A. E.; Barbara, P. F. *J. Opt. Soc. Am. B* **1990**, *7*, 1521.
(79) Lin, Y.; Jonah, C. D. *J. Phys. Chem.* **1993**, *97*, 295.
(80) Kivelson, D.; Friedman, H. *J. Phys. Chem.* **1989**, *93*, 7026.
(81) See, for example: Baxendale, J. H.; Rasburn, E. J. *J. Chem. Soc., Faraday Trans. 1* **1974**, *70*, 705.
(82) Barnett, R. N.; Landman, U.; Cleveland, C. L.; Jortner, J. *J. Chem. Phys.* **1988**, *88*, 4429.
(83) Coe, J. V.; Lee, G. H.; Eaton, J. G.; Arnold, S. T.; Sarkas, H. W.; Bowen, K. H.; Ludewigt, C.; Haberland, H.; Worsnop, D. R. *J. Chem. Phys.* **1990**, *92*, 3980.
(84) Ayotte, P.; Johnson, M. A. *J. Chem. Phys.* **1997**, *106*, 811.
(85) In the case where the electrons are generated in the pure solvent, the H_3O^+ ions that can form rapidly an encounter pair with the electrons are the geminate ones which lie quite close to their sibling electrons at the subpicosecond time scale. As was noted in ref 24, one should think in terms of a triplet instead of a pair since the OH radical and the H_3O^+ ion are only at a distance of a water molecule diameter at those times.
(86) A more complete discussion of the spectral characteristics of the $[H_3O^+{:}e^-{:}OH]$ triplet introduced in ref 24 can be found in: Pommeret, S. Ph.D. thesis, Université de Paris-Sud, Orsay, 1991.
(87) The fit that was performed without any continuous shift estimated the extinction coefficient of the "near-infrared species" to be nearly four times larger than that obtained in our standard fit and shown in Figure 6. This is in agreement with the findings of ref 86. In our standard fit, the transient spectrum of this "species" is always significantly smaller in amplitude than that of e^-_{sb}, but this is not the case anymore when the continuous blue shift of e^-_{sb} is left out.
(88) Goulet, T.; Bernas, A.; Ferradini, C.; Jay-Gerin, J.-P. *Chem. Phys. Lett.* **1990**, *170*, 492.
(89) Han, P.; Bartels, D. M. *J. Phys. Chem.* **1990**, *94*, 5824.
(90) See, for example: Madelung, O. *Introduction to Solid-State Theory*; Springer-Verlag: Berlin, 1978; pp 252−313.